



**QUEEN'S  
UNIVERSITY  
BELFAST**

## Design Method for Circularly Polarized Frequency Selective Surfaces

Zelenchuk, D., & Fusco, V. (2016). Design Method for Circularly Polarized Frequency Selective Surfaces. In *Proceedings of 10th European Conference on Antennas & Propagation (EUCAP 2016)* Institute of Electrical and Electronics Engineers Inc.. <https://doi.org/10.1109/EuCAP.2016.7481777>

**Published in:**

Proceedings of 10th European Conference on Antennas & Propagation (EUCAP 2016)

**Document Version:**

Peer reviewed version

**Queen's University Belfast - Research Portal:**

[Link to publication record in Queen's University Belfast Research Portal](#)

**Publisher rights**

© 2016 IEEE. Personal use of this material is permitted. Permission from IEEE must be obtained for all other uses, in any current or future media, including reprinting/republishing this material for advertising or promotional purposes, creating new collective works, for resale or redistribution to servers or lists, or reuse of any copyrighted component of this work in other works.

**General rights**

Copyright for the publications made accessible via the Queen's University Belfast Research Portal is retained by the author(s) and / or other copyright owners and it is a condition of accessing these publications that users recognise and abide by the legal requirements associated with these rights.

**Take down policy**

The Research Portal is Queen's institutional repository that provides access to Queen's research output. Every effort has been made to ensure that content in the Research Portal does not infringe any person's rights, or applicable UK laws. If you discover content in the Research Portal that you believe breaches copyright or violates any law, please contact [openaccess@qub.ac.uk](mailto:openaccess@qub.ac.uk).

# Design Method for Circularly Polarized Frequency Selective Surfaces

Dmitry Zelenchuk<sup>1</sup>, Vincent Fusco<sup>1</sup>

<sup>1</sup> ECIT, Queens University of Belfast, Belfast, United Kingdom, d.zelenchuk@qub.ac.uk

**Abstract**—This paper proposes a design method for the realisation of circularly polarised frequency selective surfaces (CP FSS). An equivalent circuit model for a capacitive asymmetric loop FSS is proposed. For this model a set of nonlinear design equation for CP operation is obtained. Based on space mapping of the model and full-wave simulation, a fast converging design method for CP FSS synthesis is demonstrated for the first time.

**Index Terms**—frequency selective surfaces, circular polarisation.

## I. INTRODUCTION

Frequency selective surfaces have become indispensable component of many microwave, mm-wave and submm-wave systems [1]. Due to their low insertion losses they present popular choice for quasi-optical beam splitters in feeding systems of reflector antennas, employed for such applications as satellite communications and atmosphere sounding [2].

With the development of such systems, requirements that are more stringent are being applied to FSS performance metrics with respect to insertion loss per component as well as polarization characteristics [3]. Namely polarization performance in the form of either dual-polarisation or circular polarisation (CP) operation is being more frequently required [4]. The former requires the amplitude response of both orthogonal polarizations to be identical whereas the latter adds the condition of identical phase responses.

In this paper, we present a design methodology that permits the synthesis of FSS for CP excitation based on an equivalent circuit approach. First, we formulate the design requirements for both inductive and capacitive FSS. Then based on these requirement we design a capacitive asymmetric loop FSS with aid of a quasi-analytical model. In the last section, results of the design procedure will be discussed.

## I. DESIGN REQUIREMENTS FOR CP EXCITATION

As mentioned earlier the main requirement for an FSS to operate under CP excitation is to concurrently preserve identical amplitude and phase response for both TE- and TM-polarization within a specified frequency band.

Let us first consider a circuit model for a single element FSS, presented in Fig.1. Inductive FSS can be modelled as parallel LC-resonator, and capacitive FSS as series LC-resonator. The admittance  $Y_0$  or impedance  $Z_0 = 1/Y_0$  of the resulting Floquet waveguide is defined for both TM- and TE-polarizations as follows

$$\begin{aligned} Z_0^{TE} &= \frac{1}{Y_0^{TE}} = \frac{\eta_0}{\cos \theta} \\ Z_0^{TM} &= \frac{1}{Y_0^{TM}} = \eta_0 \cos \theta \end{aligned} \quad (1)$$

where  $\eta_0$  is plane wave impedance in free space and  $\theta$  is incident angle [5].

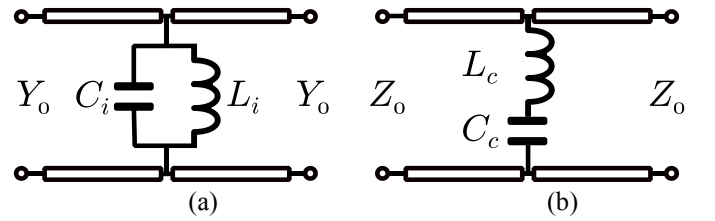


Fig. 1. FSS circuit model: (a)-inductive, (b)-capacitive.

### A. Inductive FSS

The transmission coefficient for the inductive FSS can be found from circuit theory as

$$T_i = \frac{2}{2 + Y_i/Y_0} \quad (2)$$

where  $Y_i = j\omega C_i + 1/j\omega L_i$  is the admittance of the FSS.

For CP excitation the transmission should be constrained to be identical for both TE- and TM-components, thus

$$T_i^{TE} = T_i^{TM} \quad (3)$$

It follows from (2) and (3) that

$$\frac{Y_i^{TE}}{Y_0^{TE}} = \frac{Y_i^{TM}}{Y_0^{TM}} \quad (4)$$

or substituting (1) into (4)

$$Y_i^{TE} = Y_i^{TM} \cos^2 \theta \quad (5)$$

for both inductance and capacitance the condition (5) results in

$$\begin{aligned} C_i^{TE} &= C_i^{TM} \cos^2 \theta \\ L_i^{TE} &= \frac{L_i^{TM}}{\cos^2 \theta} \end{aligned} \quad (6)$$

### B. Capacitive FSS

For capacitive FSS it is convenient to utilise the reflection coefficient

$$\Gamma_i = -\frac{1}{1 + 2Z_c/Z_0} \quad (7)$$

where  $Z_c = j\omega L_c + 1/j\omega C_c$  is the admittance of the FSS.

Now, for CP the reflection coefficient should be identical for both TE- and TM-components, thus

$$\Gamma_c^{TE} = \Gamma_c^{TM} \quad (8)$$

It follows from (7) and (8) that

$$\frac{Z_c^{TE}}{Z_0^{TE}} = \frac{Z_c^{TM}}{Z_0^{TM}} \quad (9)$$

or substituting (1) into (9)

$$Z_c^{TE} = \frac{Z_c^{TM}}{\cos^2 \theta} \quad (10)$$

for inductance and capacitance the condition (10) results in

$$\begin{aligned} C_c^{TE} &= C_c^{TM} \cos^2 \theta \\ L_c^{TE} &= \frac{L_c^{TM}}{\cos^2 \theta} \end{aligned} \quad (11)$$

It is worth noting that for inductance and capacitance situations conditions (6) and (11) are analogous.

## II. DESIGN OF ASYMMETRIC LOOP FSS

In order to design the FSS with required CP response one may apply direct optimisation of the structure with conditions (3) or (8) comprising the objective function. In some particular cases closed-form expressions exist for the inductance and capacitance, thus making possible direct synthesis with (6) or (11).

### A. Equivalent circuit for rectangular loop FSS

One of the structures with known equivalent circuit is a strip FSS and its derivatives such as grid FSS, square loop, double square loop [5]–[8]. The equivalent circuits are based on strip grating, see Fig. 2, whose impedance is given in [9]. In this paper we will employ a loop element, whose equivalent circuit corresponds to the one in Fig. 1b, in order to synthesize a bandstop FSS for CP excitation at oblique incidence.

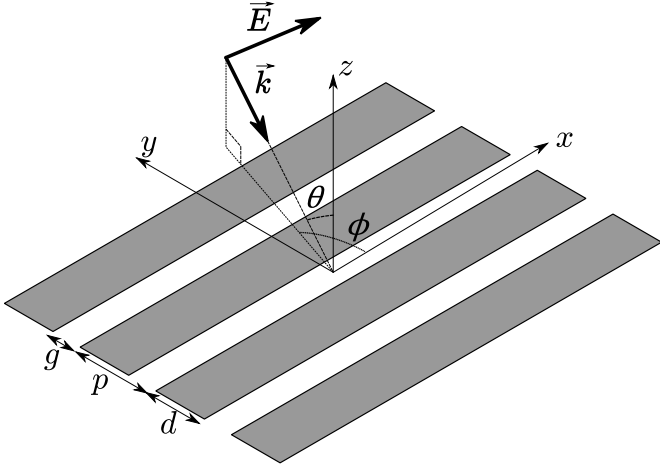


Fig. 2. Strip grating.

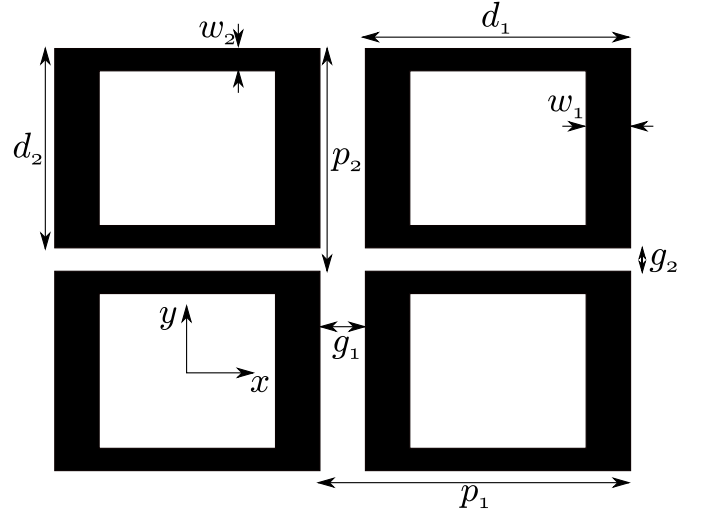


Fig. 3. Asymmetrical loop FSS.

The loop element has been made asymmetric, see Fig. 3, as upon careful study of the expressions for the symmetrical square loop [8] one comes to conclusion that for oblique incidence there is no solution satisfying conditions (11). Following the approach presented in [6]–[8] and modifying the square loop FSS impedance we obtain  $L_c^{TE,TM}$  and  $C_c^{TE,TM}$  for the asymmetric loop FSS as:

$$\begin{aligned} \tilde{X}^{TE} &= \frac{\omega L_c^{TE}}{Z_0^{TE}} = \frac{d_1}{p_1} \cos \theta F^{TE}(p_2, 2w_2, \lambda, \theta) \\ \tilde{B}^{TE} &= \frac{\omega C_c^{TE}}{Y_0^{TE}} = 4\epsilon_{eff} \frac{d_2}{p_2} \sec \theta F^{TE}(p_1, g_1, \lambda, \theta) \\ \tilde{X}^{TM} &= \frac{\omega L_c^{TM}}{Z_0^{TM}} = \frac{d_2}{p_2} \sec \phi F^{TM}(p_1, 2w_1, \lambda, \phi) \\ \tilde{B}^{TM} &= \frac{\omega C_c^{TM}}{Y_0^{TM}} = 4\epsilon_{eff} \frac{d_1}{p_1} \cos \phi F^{TM}(p_2, g_2, \lambda, \phi) \end{aligned} \quad (12)$$

where  $\lambda$  is the wavelength,  $\omega$  is the circular frequency, and  $\epsilon_{eff}$  is effective permittivity of the medium. The formulas in (12) provide good approximation for angles of incidence in the range  $p(1 + \sin \theta)/\lambda < 1$ . The number of parameters in (12) can be further reduced by noting that  $d_{1,2} = p_{1,2} - g_{1,2}$ .

Now we slightly transform the function  $F^{TE,TM}(p, g, \lambda, \theta)$  in (12)

$$F^{TE,TM}(p, g, \lambda, \theta) = p/\lambda \tilde{F}^{TE,TM}(p, g, \lambda, \theta) \quad (13)$$

where

$$\tilde{F}^{TE,TM}(p, g, \lambda, \theta) = \ln \csc(\pi g/2p) + G^{TE,TM}(p, g, \lambda, \theta) \quad (14)$$

The function above consists of two terms. The first one, theso-called grid parameter [5], does not depend on the excitation, whereas the correcting term  $G^{TE,TM}(p, g, \lambda, \theta)$  takes into account the corrections due to oblique angle excitation and thus does depend on its polarization. The function  $G^{TE,TM}(p, g, \lambda, \theta)$  can be found in [6].

### B. Design equations

The design requirements for a single element FSS should specify a resonant frequency  $f_{res}$ , bandwidth  $\Delta f$ , which can be combined into the quality factor  $Q = f_{res}/\Delta f$ , and the angle of incidence which assuming single-mode operation at the maximum frequency limits the period of the unit cell as  $p(1 + \sin \theta) < \lambda$ .

First by multiplying together the normalized susceptances and reactances for both polarization at the resonant frequency and recalling that for an  $LC$ -resonator  $\omega_{res}^2 = 1/LC$  one obtains

$$\begin{aligned} \tilde{X}^{TE} \tilde{B}^{TE} &= \frac{\omega_{res}^2 L_c^{TE} C_c^{TE}}{Z_0^{TE} Y_0^{TE}} = 1 \\ \tilde{X}^{TM} \tilde{B}^{TM} &= \frac{\omega_{res}^2 L_c^{TM} C_c^{TM}}{Z_0^{TM} Y_0^{TM}} = 1 \end{aligned} \quad (15)$$

Then by applying the formulas for the quality factor as

$$\begin{aligned} \sqrt{\frac{\tilde{X}^{TE}}{\tilde{B}^{TE}}} &= \frac{1}{Z_0^{TE}} \sqrt{\frac{L_c^{TE}}{C_c^{TE}}} = \frac{Q}{2} \\ \sqrt{\frac{\tilde{X}^{TM}}{\tilde{B}^{TM}}} &= \frac{1}{Z_0^{TM}} \sqrt{\frac{L_c^{TM}}{C_c^{TM}}} = \frac{Q}{2} \end{aligned} \quad (16)$$

two more equations are obtained.

By substituting (12)-(14) into (15) and (16) one obtains a system of four design equations

$$\begin{aligned} \tilde{F}^{TM}(p_1, 2w_1, \lambda, \phi) \tilde{F}^{TM}(p_2, g_2, \lambda, \phi) &= \frac{\lambda_{res}^2}{4\varepsilon_{eff} p_1 \left(1 - \frac{g_1}{p_1}\right) p_2 \left(1 - \frac{g_2}{p_2}\right)} \\ \tilde{F}^{TE}(p_2, 2w_2, \lambda, \theta) \tilde{F}^{TE}(p_1, g_1, \lambda, \theta) &= \frac{\lambda_{res}^2}{4\varepsilon_{eff} p_1 \left(1 - \frac{g_1}{p_1}\right) p_2 \left(1 - \frac{g_2}{p_2}\right)} \\ \sqrt{\frac{p_2 \left(1 - \frac{g_1}{p_1}\right) \cos^2 \theta \tilde{F}^{TE}(p_2, 2w_2, \lambda_{res}, \theta)}{p_1 \left(1 - \frac{g_2}{p_2}\right) 4\varepsilon_{eff} \tilde{F}^{TE}(p_1, g_1, \lambda_{res}, \theta)}} &= \frac{Q}{2} \\ \sqrt{\frac{p_1 \left(1 - \frac{g_2}{p_2}\right) \tilde{F}^{TM}(p_1, 2w_1, \lambda_{res}, \phi)}{p_2 \left(1 - \frac{g_1}{p_1}\right) 4\varepsilon_{eff} \cos^2 \phi \tilde{F}^{TM}(p_2, g_2, \lambda_{res}, \phi)}} &= \frac{Q}{2} \end{aligned} \quad (17)$$

As the periods  $p_1$  and  $p_2$  can be determined from the grating lobe condition the system of four implicit equations (17) contains four unknown geometrical parameters  $g_1$ ,  $g_2$ ,  $w_1$ , and  $w_2$ , Fig.3, and can be solved numerically.

The system of the design equations (17) has to be solved using constrained nonlinear least square minimization. In the next section, we demonstrate an example of a CP FSS design using the approach developed above.

### III. DESIGN

The design process is similar to a space mapping optimization as follows:

1) an initial FSS geometry found through minimization of the equation set (17) at given resonant frequency  $f_{sim,i}$  with appropriate constraints, e.g.  $0 < w_1 < p_1/2$ .

2) The structure with the obtained geometry is then simulated in CST Microwave Studio and its resonant frequency denoted  $f_{CST,i}$  obtained

3) Based on the difference  $f_{sim,i} - f_{CST,i}$  a new  $f_{sim,i+1}$  is found as  $f_{sim,i+1} = f_{sim,i} + (f_{sim,i} - f_{CST,i})$  and steps 1) and 2) repeated until  $f_{CST}$  is equal to the design target resonant frequency  $f_{sim,0}$ .

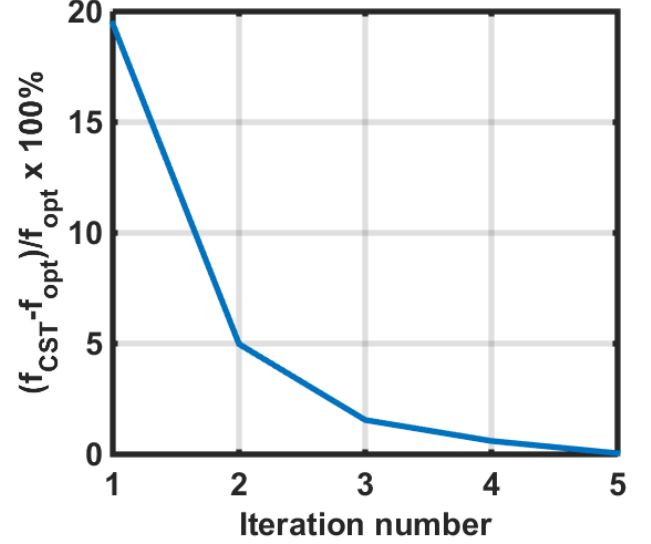


Fig. 4. Convergence of the design process.

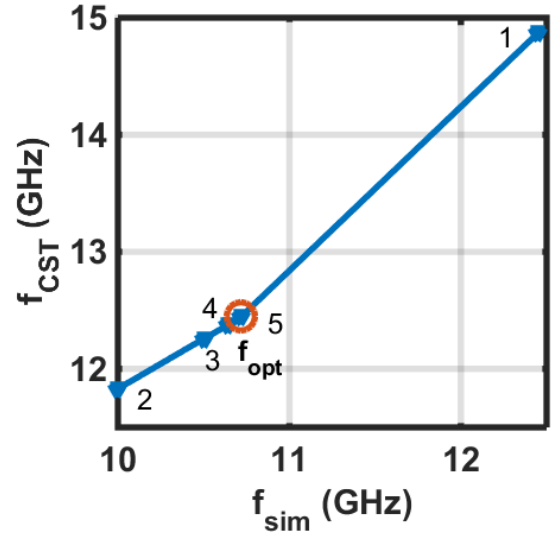


Fig. 5. Full-wave resonant frequency versus the one obtained with proposed model.

The design procedure was applied to find the geometry of a free-standing CP FSS resonating at  $f_{opt} = 12.4$  GHz with quality factor  $Q=2.45$ . The angle of incidence and period were fixed as respectively  $= 0^\circ$ ,  $\theta = 45^\circ$ ;  $p_1 = 7.2$  mm;  $p_2 = 7.2$  mm. Following the proposed design process the rest of the

geometrical parameters were found as  $w_1 = w_2 = 0.144 \text{ mm}$ ;  $g_1 = 0.8921 \text{ mm}$ ; and  $g_2 = 0.8383 \text{ mm}$ .

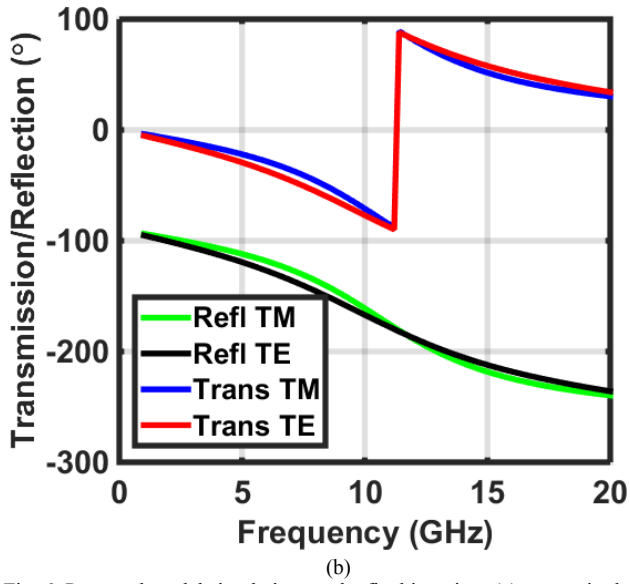
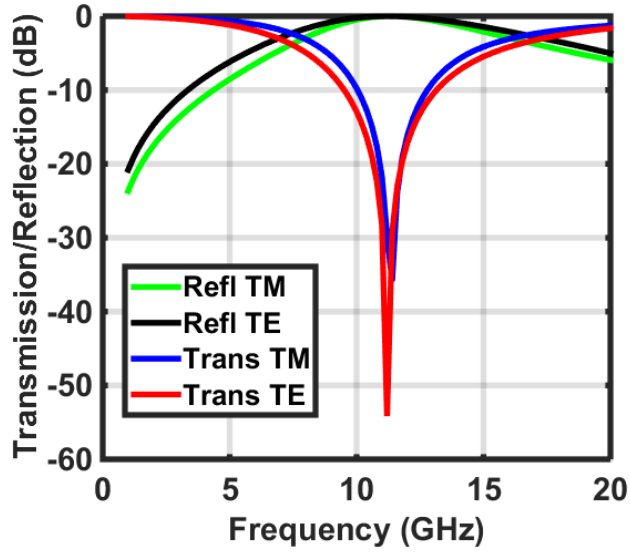


Fig. 6. Proposed model simulations at the final iteration: (a) – magnitude; (b)–phase.

The convergence of the design process is demonstrated in Fig. 4. The relative error between the resonant frequency of the full wave simulations and the optimal one, has been reduced to 0.05% in only five iterations. The functional dependence between the resonant frequencies obtained with proposed model and full-wave simulations is shown in Fig. 5. One can see that despite the non-linear mapping can be linearly approximated over short intervals with good accuracy.

One can compare the data obtained with proposed model and full-wave simulation for the optimised dimensions in Fig. 6 and Fig. 7. Here only minor frequency shift deviations occur and the behaviour of both phase and magnitude of for both TE- and

TM-polarisations is virtually identical between the approaches. This fact enables efficient space mapping and fast convergence of the design process.

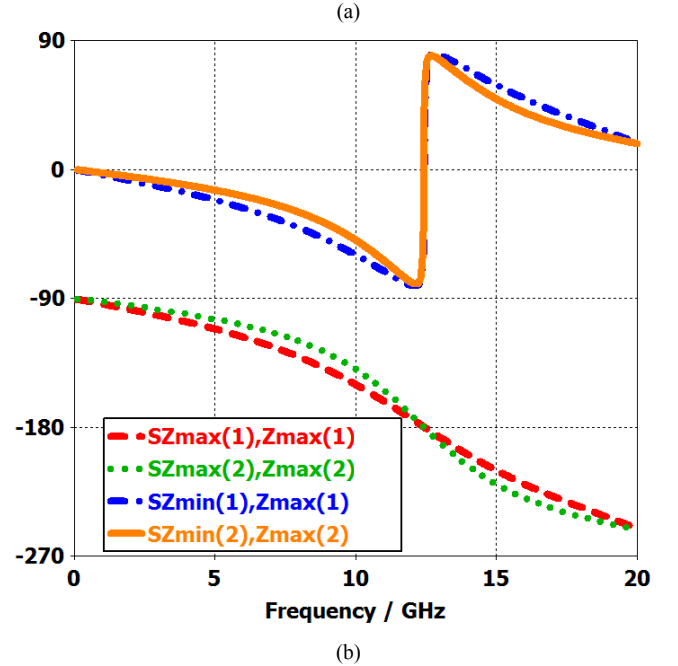
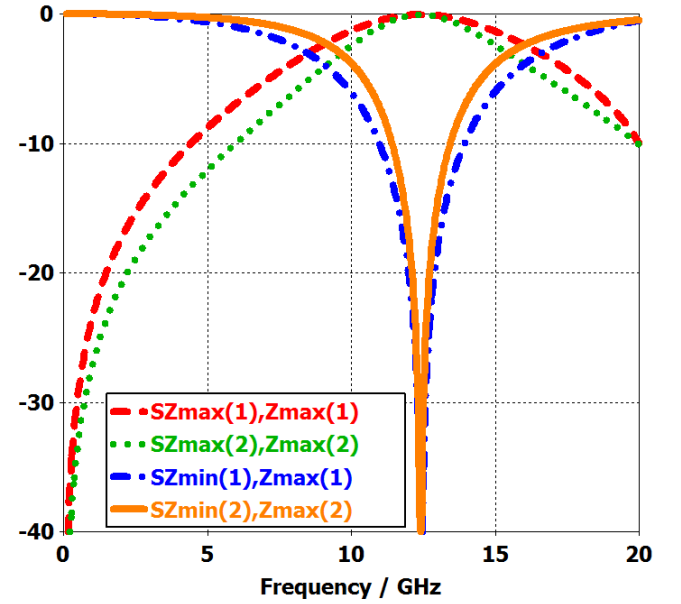


Fig. 7. Full-wave simulations at the final iteration: (a) – magnitude; (b)–phase; (1)–TM-polarisation, (2) –TE polarisation.

In order to confirm CP operation the reflection axial ratio has been plotted in Fig. 8. The axial ratio is minimal, i.e. close to zero, at the design frequency.

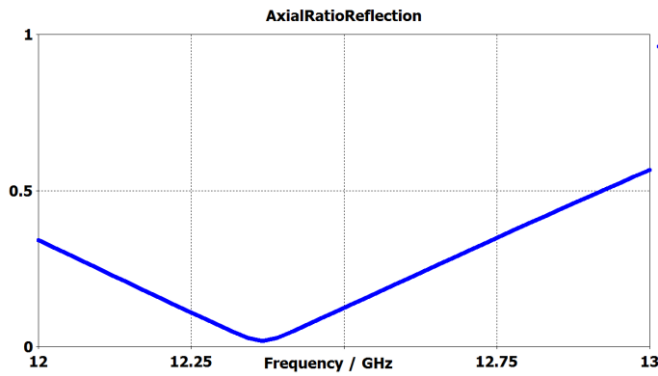


Fig. 8. Full-wave simulations of reflection axial ratio at the final iteration.

#### IV. CONCLUSION

A new design method for a CP FSS has been proposed in the paper. Based on an equivalent circuit model devised for asymmetric loop FSS, a space mapping optimisation method has been presented. Following the method, a capacitive CP FSS operating at 12.4 GHz has been designed and its performance verified using CST Microwave Studio.

#### REFERENCES

- [1] R. Dickie, P. Baine, R. Cahill, E. Doumanis, G. Goussetis, S. Christie, N. Mitchell, V. Fusco, D. Linton, J. Encinar, R. Dudley, D. Hindley, M. Naftaly, M. Arrebola, and G. Toso, "Electrical characterisation of liquid crystals at millimetre wavelengths using frequency selective surfaces," *Electron. Lett.*, vol. 48, no. 11, p. 611, 2012.
- [2] R. Dickie, R. Cahill, V. Fusco, H. S. Gamble, and N. Mitchell, "THz Frequency Selective Surface Filters for Earth Observation Remote Sensing Instruments," *IEEE Trans. Terahertz Sci. Technol.*, vol. 1, pp. 450–461, 2011.
- [3] R. Dickie, R. Cahill, H. Gamble, V. Fusco, M. Henry, M. Oldfield, P. Huggard, P. Howard, N. Grant, Y. Munro, and P. de Maagt, "Submillimeter Wave Frequency Selective Surface With Polarization Independent Spectral Responses," *IEEE Trans. Antennas Propag.*, vol. 57, pp. 1985–1994, 2009.
- [4] R. Orr, G. Goussetis, V. Fusco, R. Cahill, D. Zelenchuk, A. Pal, E. Saenz, M. Simeoni, and L. Salghetti D'roili, "Circular polarisation frequency selective surface operating in Ku and Ka band," in *Proceedings of the 8th European Conference on Antennas and Propagation (EUCAP)*, 2014, pp. 2342–2344.
- [5] O. Luukkainen, C. Simovski, G. Granet, G. Goussetis, D. Lioubtchenko, A. V. Raisanen, and S. A. Tretyakov, "Simple and Accurate Analytical Model of Planar Grids and High-Impedance Surfaces Comprising Metal Strips or Patches," *IEEE Trans. Antennas Propag.*, vol. 56, no. 6, pp. 1624–1632, Jun. 2008.
- [6] C. K. Lee and R. J. Langley, "Equivalent-circuit models for frequency-selective surfaces at oblique angles of incidence," *IEEE Proc. H Microwaves, Antennas Propag.*, vol. 132, no. 6, p. 395, 1985.
- [7] R. J. Langley and E. A. Parker, "Equivalent circuit model for arrays of square loops," *Electron. Lett.*, vol. 18, no. 7, p. 294, 1982.
- [8] A. E. Yilmaz and M. Kuzuoglu, "Design of the Square Loop Frequency Selective Surfaces with Particle Swarm Optimization via the Equivalent Circuit Model," *Radioengineering*, vol. 18, no. 2, pp. 95–102, 2009.
- [9] N. Marcuvitz, *Waveguide Handbook*, 1st ed. New York: McGraw-Hill, 1951.